International Scientific Organization
http://iscientific.org/
Chemistry International
www.bosaljournals.com/chemint/

Green synthesis of iron nanoparticles using flower extract of *Piliostigma thonningii* and their antibacterial activity evaluation

Okenwa Uchenna Igwe* and Francis Nwamezie

Department of Chemistry, Michael Okpara University of Agriculture, Umudike, P.M.B. 7267 Umuahia, Abia State, Nigeria
*Corresponding author's E. mail: okenwauigwe@gmail.com

A R T I C L E I N F O

Article type:
Research article
Article history:
Received December 2017
Accepted January 2017
January 2018 Issue
Keywords:
Iron nanoparticles
P. thonningii
FTIR
SEM
XRD
Antibacterial activity

A B S T R A C T

Iron nanoparticles have gained tremendous attention due to their application in magnetic storage media, ferrofluids, biosensors, catalysts, separation processes, environmental remediation and antibacterial activity. In the present paper, iron nanoparticles were synthesized using aqueous flower extract of *Piliostigma thonningii*, a natural nontoxic herbal infusion. Iron nanoparticles were generated by reaction of ferrous chloride solution with the flower extract. The reductants present in the flower extract acted as reducing and stabilizing agents. UV-vis analysis of the iron nanoparticles showed continuous absorption in the visible range suggesting the iron nanoparticles were amorphous. This was confirmed by X-ray diffraction (XRD) analysis which did not have distinct diffraction peaks. Scanning electron microscopy (SEM) analysis revealed that the synthesized iron nanoparticles were aggregated as irregular clusters with rough surfaces. FT-IR studies showed the functional groups that participated in the bio-reduction process to include a C-H stretch (due to alkane CH_3, CH_2 or CH), C=O stretch (due to aldehydes), O-H bend (due to *tert*-alcohol or phenol), C-O stretch (due to aldehydes or phenols) and C-O stretch (due to alcohols) corresponding to absorptions at 2929.00, 1721.53, 1405.19, 1266.31 and 1030.02 cm^{-1} respectively. The iron nanoparticles showed significant antibacterial activity against *Escharichia coli* and *Staphylococcus aureus* suggesting potential antibacterial application.

Capsule Summary: Iron nanoparticles synthesized using aqueous flower extract of *P. thonningii* were characterized using UV-vis, FTIR, SEM, and XRD techniques and were found to be amorphous, however, they showed appreciable antibacterial activity.

Cite This Article As: O. U. Igwe and F. Nwamezie. Green synthesis of iron nanoparticles using flower extract of *Piliostigma thonningii* and antibacterial activity evaluation. Chemistry International 4(1) (2018) 60-66.

INTRODUCTION

Nanoparticles have excellent recognition and acceptance due to their desirable characteristic features some of which include catalytic, optical, magnetic, and electrical properties. These particles possess remarkably new properties when compared to their bulk counterpart (Singh et al., 2011). This means that nanoparticles do not necessarily behave in the same manner as larger particles in chemical reactions, but tend to be much more reactive. The particles possess an enormous amount of energy in their high surface-to-volume ratios, which changes their reactivity. Nanoparticles have a general tendency to adsorb species very readily, which has obvious kinetic advantages (Huber, 2005).

Iron nanoparticles are of great importance in a wide range of applications, including magnetic storage media, ferrofluids, biosensors, catalysts, separation processes and environmental remediation (Jeyadevan et al., 2003; Zhang et al., 2005; Guo et al., 2012; Mahdavi et al., 2013). As a result of their unique physical, chemical, thermal, and mechanical properties, and also by having suitable surface characteristics, super-paramagnetic nanoparticles offer a great potential in many biomedical applications, such as cellular therapy, tissue repair, drug delivery, magnetic resonance imaging (MRI), hyperthermia, and magnetofection (Guo et al., 2012; Mahdavi et al., 2013). Up till date, numerous methods have been developed for the manufacture of iron nanoparticles, including chemical vapour deposition, inert gas condensation, pulsed laser ablation, spark discharge generation, sputtering gas-aggregation, thermal decomposition, thermal reduction of oxide compounds, hydrogenation of metallic complexes and the aqueous reduction of iron salts (Crane and Scott, 2012). These processes are via either chemical or physical means. Chemical synthesis methods lead to presence of some toxic chemicals absorbed on the surface that may have adverse effect in the medical application.

The biosynthesis of nanoparticles has been proposed as a cost effective environmental friendly alternative to chemical and physical methods. Consequently, nanomaterials have been synthesized using microorganisms and plant extracts (Awwad and Salem, 2012).

The bioreduction of metal nanoparticles by combinations of biomolecules found in plant extracts such as enzymes, proteins, amino acids, vitamins, polysaccharides, typically obtained by contact of a broth of plant with metal salts, has been intensively investigated in recent years (Iravani, 2011; Shah et al., 2014). This method of synthesis also known as 'green synthesis' provides advancement over chemical and physical method as it is cost effective, environment friendly, easily scaled up for large scale synthesis and in this method there is no need to use high pressure, energy, temperature and toxic chemicals (Jain et al., 2009).

Piliostigma thonningii Schum is a leguminous plant that belongs to the *Caesalpinioideae* family (Kwaji et al., 2010). *P. thonningii* leaves have been reported to be used in traditional medicine, especially in the treatment of malaria, wounds, ulcers, gastric/heart pain, gingivitis, fever, haemorrhoids and backache (Burkill, 1995).

Due to environmental problems associated with other methods of nanoparticles synthesis, this paper's objective is to synthesize iron nanoparticles through an eco-friendly method. Herein is therefore reported the green synthesis of iron nanoparticles using flower extracts of *Piliostigma thonningii* and their antibacterial activity evaluation.

MATERIAL AND METHODS

Collection of plant materials

Fresh flowers of *P. thonningii* were collected from the tree plants within the campus of Michael Okpara University of Agriculture, Umudike, Abia State, Nigeria, where they are planted as ornamental trees. The flower materials weighed 40 g. After identification of the plant material at the Taxonomy Section of Forestry Department of the aforementioned university, it was subjected to aqueous and methanol extractions.

Preparation of aqueous plant extract

The collected flowers were thoroughly washed under running tap water and rinsed severally with distilled water followed by sun-drying to remove residual moisture. The dried materials were cut into fine pieces and dispersed in 200 ml of sterile distilled water in a 500 ml glass beaker and boiled at 80 °C for 15 min. and were allowed to cool. After that, the solution was filtered through Whatman No. 1 filter paper (Springfield Mill. Maidstone. Kent, England) and the filtrate was used immediately for the synthesis of iron nanoparticles.

Synthesis of iron nanoparticles

For the synthesis of iron nanoparticles, 10 ml of the aqueous flower extract was added to 90 ml of 1×10^{-3} M aqueous $FeCl_2$ solution in a 250 ml Erlenmeyer flask. Within 2 minutes, change in colour was observed from brown to brick red indicating the formation of iron nanoparticles. The iron nanoparticles solution obtained was purified by repeated centrifugation at 10000 rpm for 15 min. followed by re-dispersion of the pellet in deionized water. The iron nanoparticles were dried in an oven at 80 °C and then stored in a container.

Ultraviolet-visible spectroscopy analysis

The bio-reduction process of iron ions in aqueous solution was measured by sampling of 1 ml aliquot compared with 1 ml of distilled water used as blank and subsequently measuring UV-visible spectrum of the solution. UV-visible spectrum was monitored on Shimadzu dual beam spectrophotometer (Model, UV-2500PC Series) operated at a width slit of 2 nm within the wavelength range of 200 to 800 nm.

Fourier transform infrared spectroscopy analysis

This was carried out on *P. thonningii* flower extract and on the iron nanoparticles. FT-IR measurement of the samples were performed using FTIR-8400S Fourier Transform Infrared Spectrophotometer, Shimadzu, Japan, in a diffused reflectance mode at a resolution of 4 cm^{-1} in potassium bromide (KBr) pellets in the wave number range of 4500-250 cm^{-1}.

Scanning electron microscopy analysis

Morphology of the nanoparticles was studied using SEM analysis (MODEL -PHENOM ProX Scanning Element Microscope manufactured by PhenomWorld Eindhoven, the Netherlands).

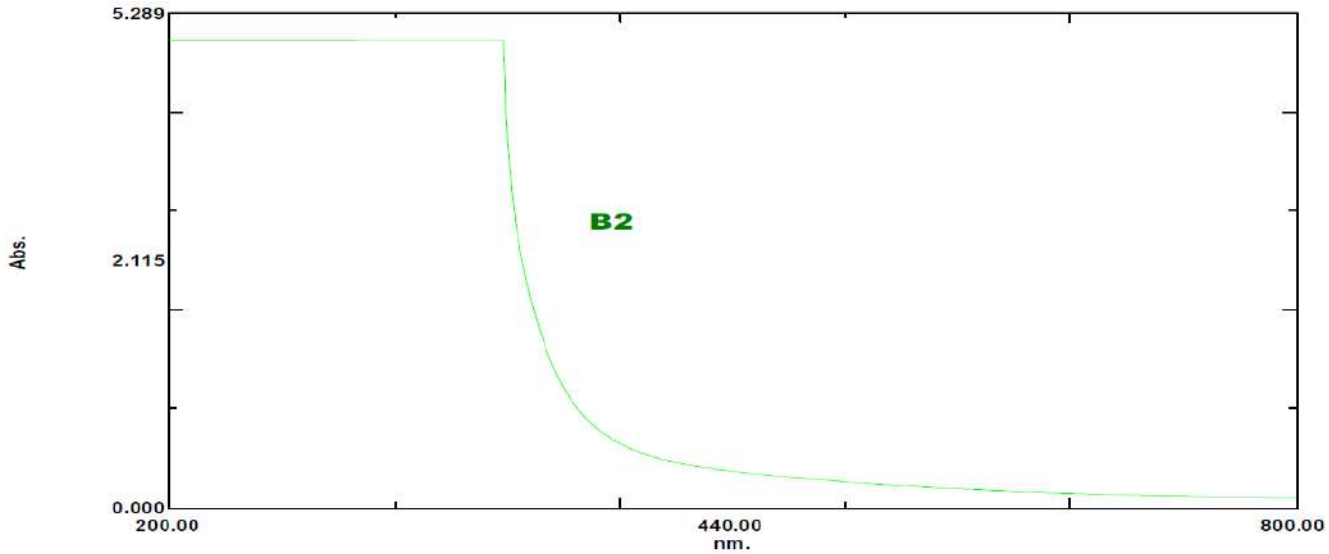

Fig. 1: UV-vis absorption spectrum of iron nanoparticles synthesized using *P. thonningii* flower extract.

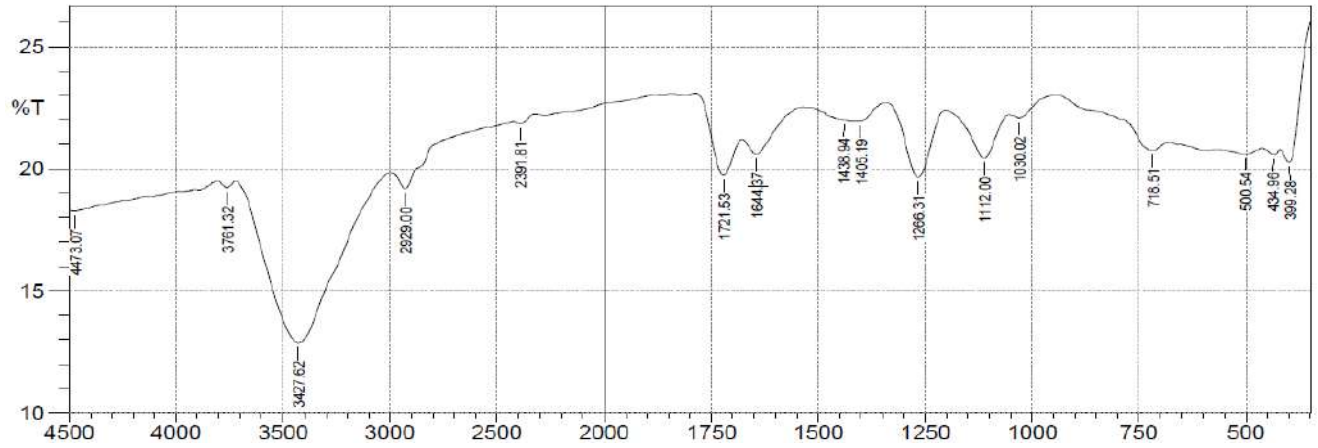

Fig. 2: FT-IR of *P. thonningii* flower extract (X and Y axes are wavenumber (cm^{-1}) and % Transmittance respectively)

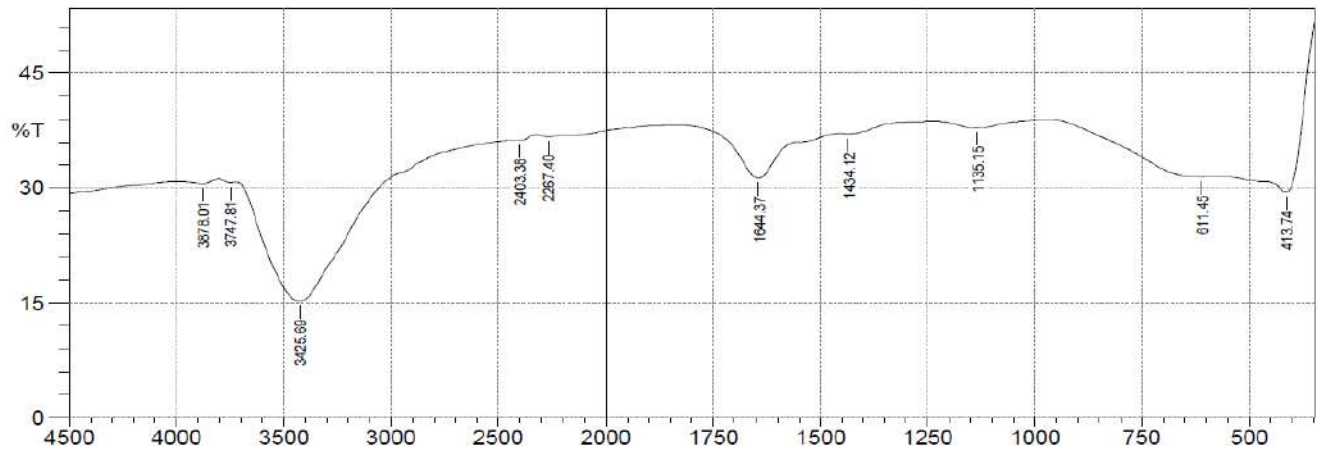

Fig. 3: FT-IR spectrum of iron nanoparticles synthesized using *P. thonningii* flower extract (X and Y axes are wavenumber (cm^{-1}) and % Transmittance respectively)

Table 1: FT-IR absorption peaks and intensities of *P. thonningii* flower extract

Peak (cm^{-1})	Functional Group
3427.62	O-H stretch due to alcohols or phenols
2929.00	C-H stretch due to alkane CH_3, CH_2 or CH
1721.53	C=O stretch due to aldehydes
1644.37	C=C stretch of alkenes
1438.94	C-H bend due to CH_3, CH_2 or CH
1405.19	O-H bend due to *tert*-alcohol or phenol
1266.31	C-O stretch due to aldehydes or phenols
1112.00	C-O stretch due to alcohols
1030.02	C-O stretch due to alcohols

Table 2: FT-IR absorption peaks and intensities of iron nanoparticles synthesized using *P. thonningii* flower extract

Peak (cm^{-1})	Functional Group
3425.69	O-H stretch due to alcohols or phenols
1644.37	C=C stretch of alkenes
1434.12	C-H bend due to CH_3, CH_2 or CH
1135.15	C-O stretch due to alcohols

Table 3: Antibacterial activity of iron nanoparticles synthesized using flower extract of *P. thonningii*

Bacterial strains	Zone of inhibition (mm)	MIC (%)	Positive standard GT (mm)
E. coli	21.8 ± 0.2	20	22.2 ± 0.3
S. aureus	20.2 ± 0.2	25	21.5 ± 0.5

Notes: Values are in mm and include the diameter of the paper disc (5 mm) and are expressed as mean of triplicate results ± standard deviation; MIC, minimum inhibitory concentration; GT, gentamycine.

X-ray diffraction analysis

XRD (PANanalytical, Netherlands) patterns were obtained with a diffractometer (Empyrean model, Netherlands) using Cu-Kα radiation of wavelength (λ) = 1.541 Å. The sample was made smoother and was imparted on a slide which was then charged into the machine after adjusting the machine parameters and was operated via a monitor.

Antibacterial activity screening

The *in vitro* antibacterial activity of the iron nanoparticles was carried out for 24 h culture of two selected bacteria. The bacteria organisms used were *Escherichia coli* (Gram-negative) and *Staphylococcus aureus* (Gram-positive). The test organisms were clinical isolates of human pathogens obtained from stock cultures at the Federal Medical Centre, Umuahia, Abia State, Nigeria. Circular paper discs of 5 mm diameter were cut from Whatman No 1 filter paper using office paper perforator. After boiling the paper discs in distilled water for an hour (in order to remove any residual preservatives), they were allowed to drain dry and were wrapped in aluminium foil and sterilized in an autoclave at 121 °C for 15 min. They were however used within 48 h of production (Igwe, 2015). The sensitivity of each test microorganism to the iron nanoparticles was determined using the Disc Diffusion Technique (Pelczar and Chan, 1977). A loopful of each test sample organism was aseptically transferred into the surface of a sterile solid medium, appropriate for the test organism. Using a flamed glass hockey, the inoculum was spread evenly over the surface of the medium, and then with the aid of a flamed pair of forceps, the iron nanoparticles bearing paper discs were carefully placed on the surface of the inoculated medium at some distance from one another. The inoculated plates were incubated for 24 h in an incubator at 37 °C. They were examined daily for growth and for the presence of inhibition zones around the paper discs. The level of sensitivity was determined by the diameter of the inhibition zone as measured with a transparent millimetre rule. Gentamycine was used as a standard antibacterial drug. The minimum inhibitory concentration (MIC) was determined by comparing the different concentrations of the sample having different zones and selecting the lowest concentration.

RESULTS AND DISCUSSION

On adding ferrous chloride solution to the aqueous *P. thonningii* flower extract, within 2 min. the solution turned from brown to brick red, indicating the formation of iron nanoparticles. The UV-vis spectrum of iron nanoparticles

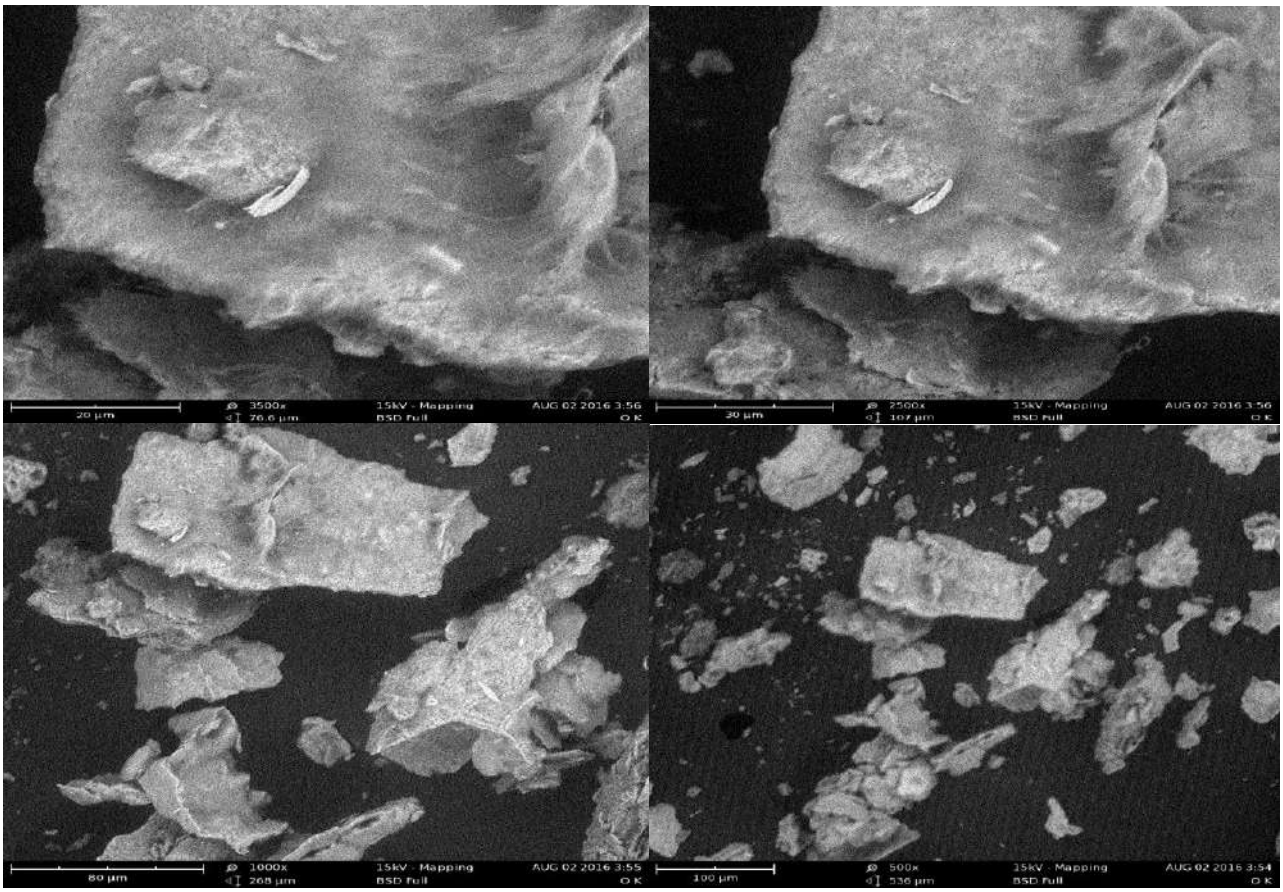

Fig. 4: SEM images of iron nanoparticles synthesized using flower extract of *P. thonningii* at different levels of magnification

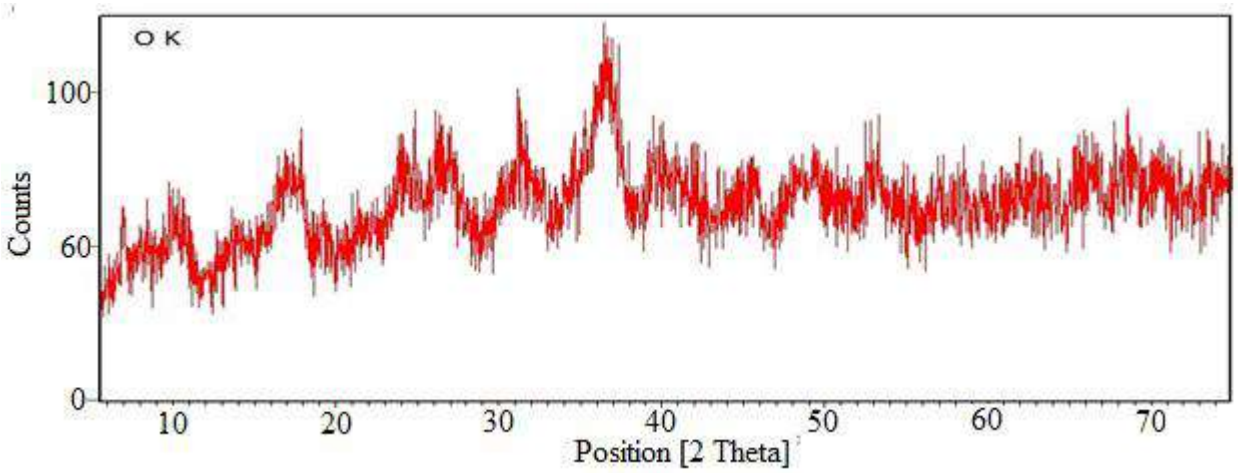

Fig. 5: XRD patterns of iron nanoparticles synthesized using flower extract of *P. thonningii*

synthesized using aqueous *P. thonningii* flower extract showed continuous absorption in the visible range (Fig. 1). Nadagouda et al. (2010) and Njagi et al. (2011) obtained similar UV-vis spectra for amorphous iron nanoparticles synthesized using aqueous tea extracts and sorghum bran extracts respectively. This suggests that the iron nanoparticles synthesized here might be amorphous.

FT-IR spectroscopy was used to assess the functional groups that participated in the reduction of iron ions to iron nanoparticles. Figs. 2 and 3 show the FT-IR spectra of *P. thonningii* flower extract and that of the iron nanoparticles

bio-synthesized from it, respectively, while the interpretations of the peaks are shown in Tables 1 and 2 respectively. Some absorptions found in the spectrum of the extract are absent in the spectrum of iron nanoparticles shown above. These absorptions are at 2929.00, 1721.53, 1405.19, 1266.31 and 1030.02 cm^{-1} corresponding to C-H stretch (due to alkane CH_3, CH_2 or CH), C=O stretch (due to aldehydes), O-H bend (due to *tert*-alcohol or phenol), C-O stretch (due to aldehydes or phenols) and C-O stretch (due to alcohols) respectively. The absence or disappearance of these functional groups in the spectrum of iron nanoparticles (Fig. 3) is an indication that a chemical change occurred and that these groups were involved in the bio-reduction of iron ions to iron nanoparticles followed by stabilization of the nanoparticles. Also, the existence of O-H, C=C, C-H and C-O groups in the nanoparticles suggested that the surface of the nanoparticles were associated with compounds whose chemical nature comprised these groups. The O-H group might also be as a result of water molecules that adhered to the nanoparticles surface.

The iron nanoparticles were analyzed for structure and morphology using SEM at different magnification levels (Fig. 4). SEM images revealed that the synthesized iron nanoparticles were aggregated as irregular rectangular, rod-like and spherical shapes with rough surfaces. Simply put, these images suggest that the particles agglomerate to form irregular clusters. The clusters were formed in the diameter range of 20 to 100 µm.

The XRD patterns of iron nanoparticles did not have distinct diffraction peaks, suggesting the amorphousness of the synthesized iron nanoparticles (Fig. 5). This had earlier been demonstrated by the UV-visible analysis of the iron nanoparticles in Fig. 1 where continuous absorption in the visible range was observed. This observation is in agreement with that reported by Nadagouda et al. (2010) and Njagi et al. (2011) for amorphous iron nanoparticles.

The antibacterial activity of the iron nanoparticles was tested against *E. coli* (Gram-negative bacteria) and *S. aureus* (Gram-positive bacteria). The results are shown in Table 3. From the experiment it was observed that the iron nanoparticles were effective in inhibiting bacterial growth. The zone of inhibition of 21.8 ± 0.2 mm was observed for *E. coli* while 20.2 ± 0.3 mm was observed for *S. aureus*. These values were just a little below the values obtained for the standard (gentamycine). The low MIC values of 20 and 25 % indicate a high antibacterial potency of the iron nanoparticles.

The antimicrobial activity of iron nanoparticles has not been adequately reported. The antibacterial activity of iron nanoparticles towards Gram-negative bacteria was higher when compared to Gram-positive bacteria. The difference in activity against these two types of bacteria could be as a result of differences in structure and composition of the cell membrane (Padil and Černík, 2013). Gram-positive bacteria have thicker peptidoglycan cell membranes compared to the Gram-negative bacteria (Liang, 2012) and so it would be more difficult for iron nanoparticles to penetrate it, resulting in a low antibacterial response. The differential sensitivity of bacteria towards iron nanoparticles depends upon particle size, bacterial cell wall structure, and the degree of contact between organisms and nanoparticles.

CONCLUSIONS

The green method of iron nanoparticles synthesis adopted here is simple, cost effective and environmentally friendly. The synthesized iron nanoparticles were found to be stable but formed aggregates with irregular morphology as shown by the SEM. UV-vis and XRD studies confirmed the iron nanoparticles to be amorphous. Functional groups directly involved in the bio-reduction of iron ions to zero-valent iron nanoparticles were studied using FT-IR analysis. The antibacterial activity experiment performed on *E. coli* and *S. aureus* clearly demonstrated that the synthesized iron nanoparticles have high antibacterial effects. Significant antibacterial action was shown on both the Gram classes of bacteria used. These nanoparticles could find application in the management of diseases caused by these pathogens.

ACKNOWLEDGEMENT

The authors are grateful to Mr. I. K. Ndukwe of Plant Taxonomy Section, Forestry Department, Michael Okpara University of Agriculture, Umudike, for identifying and authenticating the plant sample.

REFERENCES

Awwad, A.M., Salem, N.M., 2012. A green and facile approach for synthesis of magnetite nanoparticles. Journal of Nanoscience and Nanotechnology 2(6), 208-2013.

Burkill, H.M., 1995. The useful plants of West tropical Africa. Royal Botanical Gardens, Kew., 2nd ed., Vol. 3.pp. 50.

Crane, R.A., Scott, T.B., 2012. Nanoscale zero-valent iron: Future prospects for an emerging water treatment technology. Journal of Hazardous Materials 211, 112-125.

Guo, J., Wanga, R., Tjiu, W.W., Pan, J., Liu, T., 2012. Synthesis of Fe nanoparticles@graphene composites for environmental applications. Journal of Hazardous Materials 225, 63-73.

Huber, D.L., 2005. Synthesis, properties and applications of iron nanoparticles. Small 1(5), 482-501.

Igwe, O. U., 2015. Chemical constituents of the leaf essential oil of *Carica papaya* from South East Nigeria and its antimicrobial activity. International Journal of Research in Pharmacy and Chemistry 5(1), 77-83.

Iravani, R., 2011. Green synthesis of metal nanoparticles using plants. Green Chemistry 13, 2638-2650.

Jain, D., Daima, H.K., Kachhwaha, S., Kothari, S.L., 2009. Synthesis of plant-mediated silver nanoparticles using papaya fruit extract and evaluation of their antimicrobial activities. Digest Journal of Nanomaterials and Biostructures, 4(3), 557-563.

Jeyadevan, B., Chinnasamy, C.N., Shinoda, K., Tohji, K., Oka, H., 2003. Mn-Zn ferrite with higher magnetization for temperature sensitive magnetic fluid. Journal of Applied Physics 93, 8450-8452.

Kwaji, A., Bassi, P.U., Aoill, M., Nneji, C.M., Ademowo, G., 2010. Preliminary studies on *Piliostigma thonningii* Schum leaf extract: Phytochemical screening and *in vitro* antimalarial activity. African Journal Microbiology Research 4(9), 735-739.

Liang, X., Sun, M., Li, L., Qiao, R., Chen, K., Xiao, Q., Xu, F., 2012. Preparation and antibacterial activities of polyaniline/$Cu_{0.05}Zn_{0.95O}$ nanocomposites. Dalton Transactions 41(9), 2804-2811.

Mahdavi, M., Namvar, F., Ahmad, M.B., Mohamad, R., 2013. Green biosynthesis and characterization of magnetic iron oxide (Fe_3O_4) nanoparticles using seaweed (*Sargassum muticum*) aqueous extract. Molecules 18, 5954-5964.

Nadagouda, M.N., Castle, A.B., Murdock, R.C., Hussain, S.M., Varma, R.S., 2010. In vitro biocompatibility of nanoscale zerovalent iron particles (NZVI) synthesized using tea polyphenols. Green Chemistry 12, 114-122.

Njagi, E.C., Huang, H., Stafford, L., Genuino, H., Galindo, H.M., Collins, J.B., Hoag, G.E., Suib, S.L., 2011. Biosynthesis of iron and silver nanoparticles at room temperature using aqueous sorghum bran extracts. Langmuir 27(1), 264–271.

Padil, V.V.T., Černík, M., 2013. Green synthesis of copper oxide nanoparticles using gum karaya as a biotemplate and their antibacterial application. International Journal of Nanomedicine 8, 889-898.

Pelczar, M., Chan, E.C.S., 1977. Laboratory exercises in microbiology. Black Dot Inc. New York, pp 425.

Shah, S., Dasgupta, S., Chakraborty, M., Vadakkekara, R., Hajoori, M., 2014). Green synthesis of iron nanoparticles using plant extracts. International Journal of Biological and Pharmaceutical Research 5(6), 549-552.

Singh, R.P., Magesh, S., Rakkiyappan, C., 2011. Ginger *(Zingiber officinale)* root extract: a source of silver nanoparticles and their application. International Journal of Bio-Engineering Sciences and technology 2(3), 75-80.

Zhang, J.L., Wang, Y., Ji, H., Wei, Y. G., Wu, N.Z., Zuo, B.J., Wang, Q.L., 2005. Magnetic nanocomposite catalysts with high activity and selectivity for selective hydrogenation of *ortho*-chloronitrobenzene. Journal of Catalysis 229, 114-118.

Visit us at: http://bosaljournals.com/chemint/
Submissions are accepted at: editorci@bosaljournals.com